Journal of Microbiology (2024) 62:727–737
https://doi.org/10.1007/s12275-024-00151-y

EVOLUTIONARY MICROBIOLOGY AND SYSTEMATICS

Pannonibacter tanglangensis sp. nov., a New Species Isolated from Pond Sediment

Lei Wang[1] · Yanpeng Cheng[2] · Panpan Yang[1,3] · Jinjin Zhang[4] · Gui Zhang[5] · Sihui Zhang[6] · Jing Yang[7,8] · Zhen Zhang[2] · Lulu Hu[1] · Ji Pu[7] · Yanying Yang[9] · Xin-He Lai[10] · Jianguo Xu[6,7,8] · Yinghui Li[1] · Qinghua Hu[1]

Received: 12 March 2024 / Revised: 2 June 2024 / Accepted: 9 June 2024 / Published online: 5 July 2024

Abstract

Two bacterial strains (XCT-34^T and XCT-53) isolated from sediment samples of an artificial freshwater reservoir were analyzed using a polyphasic approach. The two isolates are aerobic, Gram-stain-negative, oxidase-negative, catalase-positive, motile with polar flagella, rod-shaped, and approximately 1.4–3.4 × 0.4–0.9 μm in size. Phylogenetic analyses based on 16S rRNA gene and whole-genome sequences showed that the two strains formed a distinct branch within the evolutionary radiation of the genus *Pannonibacter*, closest to *Pannonibacter carbonis* Q4.6^T (KCTC 52466). Furthermore, lower than threshold average nucleotide identity values (ANI, 85.7–86.4%) and digital DNA–DNA hybridization values (dDDH, 22.3–30.5%) of the two strains compared to the nearest type strains also confirmed that they represented a novel species. Genomic analyses, including annotation of the KEGG pathways, prediction of the secondary metabolism biosynthetic gene clusters and PHI phenotypes, supported functional inference and differentiation of the strains from the closely related taxa. Results of chemotaxonomic and physiological studies revealed that their distinct phenotypic characteristics distinguished them from existing *Pannonibacter* species. Thus, the two strains are considered to represent a novel species of *Pannonibacter*, for which the name of *Pannonibacter tanglangensis* sp. nov. is proposed, with XCT-34^T (= KCTC 82332^T = GDMCC 1.1947^T) as the respective type strain.

Keywords New species · *Pannonibacter* · *Pannonibacter tanglangensis* sp. nov.

Lei Wang and Yanpeng Cheng contributed equally to this work.

✉ Yinghui Li
30913142@qq.com

✉ Qinghua Hu
huqinghua03@163.com

[1] Microbiology Laboratory, Shenzhen Center for Disease Control and Prevention, Shenzhen 518000, China

[2] Division of Communicable Disease Control and Prevention, Shenzhen Center for Disease Control and Prevention, Shenzhen 518000, China

[3] School of Public Health, Shanxi Medical University, Taiyuan 030001, China

[4] Division of Quality and Management, Futian District Center for Disease Control and Prevention, Shenzhen 518000, China

[5] Infection Management Office, Shandong Provincial Hospital Affiliated to Shandong First Medical University, Jinan 250021, China

[6] Department of Laboratorial Science and Technology and Vaccine Research Center, School of Public Health, Peking University, Beijing 100191, China

[7] State Key Laboratory of Infectious Disease Prevention and Control, National Institute for Communicable Disease Control and Prevention, Chinese Center for Disease Control and Prevention, Beijing 102206, China

[8] Research Units of Discovery of Unknown Bacteria and Function, Chinese Academy of Medical Sciences, Beijing 102206, China

[9] Department of Endemic Disease Prevention and Control, Qinghai Institute for Endemic Disease Prevention and Control, Xining 810000, China

[10] Shenzhen Boya Gene Technology Company Limited, Shenzhen 518107, China

Introduction

Pannonibacter phragmitetus, the type species of the genus *Pannonibacter* within the *α*-subclass of the *Proteobacteria,* was isolated in 2003 from the surface of decomposing reed rhizomes in Lake Fertő (Borsodi et al., 2003). Members of this genus are Gram-stain-negative, motile, straight to slightly curved rods, with Q-10 as the predominant menaquinone and $C_{18:1}\omega7c$ as the primary fatty acid. At the time of writing, the only three members of the genus with validly published names (https://lpsn.dsmz.de/genus/pannonibacter) are *P. carbonis* (Xi et al., 2018), *P. indicus* (Bandyopadhyay et al., 2013), and *P. phragmitetus* (Borsodi et al., 2003). All *Pannonibacter* species were isolated from extreme environments, such as coal mine water (Xi et al., 2018), hot-spring sediment (Bandyopadhyay et al., 2013) and alkaline lake (Borsodi et al., 2003), suggesting that they are extremophiles. Previous studies have indicated that *Pannonibacter* strains were highly alkaline- (Bandyopadhyay et al., 2013; Borsodi et al., 2003; Xi et al., 2018), chromium- (Shi et al., 2012) or arsenate-tolerant (Bandyopadhyay & Das, 2016) bacteria. Tolerance to extreme environments in *Pannonibacter* species was due to the presence of certain exceptional biological functions, such as physiological responses to the reduction of Cr(VI), the adsorption of Pb(II) (Liao et al., 2020) or the removal of toxic lead (Saravanan et al., 2021). Furthermore, it had been shown that *P. phragmitetus* was associated with human infectious diseases, as this species was isolated from human blood cultures (Holmes et al., 2006) and also identified in a clinical sample of a bacteremic patient (Gallardo et al., 2020). We specifically chose the sediment samples from a pond located in a suburban park near the Tanglang Mountain in Shenzhen of China to study bacterial diversity. In this study we analyzed the two novel strains (XCT-34^T, XCT-53) via a polyphasic taxonomic approach and propose that they represent a new species of the genus *Pannonibacter*.

Materials and Methods

Isolation and Culture

Sediment samples were collected in May 2018 from the bottom surface layer (depth of 10–15 cm) of a pond located around the Tanglang mountain in Shenzhen of China. Briefly, sediment samples were collected into sterile tubes, placed in an icebox, transported to the laboratory within 2 h and stored in a freezer (− 80 °C). After thawing samples at room temperature, one gram of each sample was serially diluted in 1% sterile PBS, plated on Brain Heart Infusion (BHI) agar and Reasoner's 2A (R2A) agar plates (HiMedia), and the plates were incubated at 20–40 °C for 3–5 days under aerobic conditions. Two separate pure cultures (hereafter XCT-34^T and XCT-53) were isolated from two different sediment samples (XCT-34^T from sample No. 3, 22°34′13″N/113°59′16″E; XCT-53 from sample No. 5, 22°34′15″N/113°59′18″E) and subjected next to 16S rRNA gene sequence analysis. Strain XCT-34^T had been deposited in the Guangdong Microbial Culture Collection Center (GDMCC) and Korean Collection for Type Cultures (KCTC), with the deposit numbers of GDMCC 1.1947 and KCTC 82332, respectively.

16S rRNA Phylogeny

To genetically characterize the isolates, the nearly complete 16S rRNA gene sequence of each strain was PCR-amplified and sequenced with universal primers 27F (5′-AGA GTT TGA TCM TGG CTC AG-3′) and 1492R (5′-GGY TAC CTT GTT ACG ACT T-3′) (Delgado et al., 2006; Jin et al., 2013). Then, we submitted the 16S rRNA gene sequence to EzBioCloud (https://www.ezbiocloud.net) (Yoon et al., 2017a), a high quality database of 16S rRNA sequences, to obtain preliminary indications of a suspected new bacterial species (with a similarity below 98.7% to the closest known species). Phylogenetic tree was constructed with three algorithms (Neighbor-Joining, NJ; Maximum-Likelihood, ML; and Maximum-Parsimony, MP) using MEGA version 11 software (http://www.megasoftware.net) (Kumar et al., 2016) with a bootstrap analysis (1000 replications) as an estimation of grouping stability (Kimura, 1980). Kimura's two-parameter model was used to calculate the evolutionary distance matrices.

Whole-Genome Sequencing and Phylogenomic Analyses

In order to do complete 16S rRNA gene and the whole genome analyses, genomic DNA of the two suspected new bacterial species was extracted using a Wizard Genomic DNA purification kit (Promega) (Jin et al., 2013). The genome of strain XCT-34^T was sequenced by the Single Molecule Real-Time (SMRT) technology on the PacBio Sequel platform, assembled by SOAP*denovo,* and analyzed using the HGAP v4 application (Pacific Biosciences, SMRT Link 6.0) (Tamura et al., 2021). Meanwhile, strain XCT-53 was sequenced on the Illumina sequencing platform. The full-length sequence of the 16S rRNA gene was extracted using the RNAmmer-1.2 software and resubmitted to EzBioCloud database, searching for closest phylogenetic neighbors using BLAST algorithm (Lagesen et al., 2007).

To verify their phylogenetic position within the genus *Pannonibacter*, a phylogenomic tree was constructed by clustering and aligning the 945 core genes in MAFFT using the approximate ML algorithm in FastTree (Price et al., 2009), and visualized in Dendroscope 3 (Huson & Scornavacca, 2012). Because only 19 genomes of the 34 closest species were available in the public database for the 16S rRNA gene analysis, the core genes were determined based on 22 genome sequences which included those of the two isolates, three validated species in the genus *Pannonibacter*, and 16 closest strains from the EzTaxon database, plus *Breoghania corrubedonensis* UBF-P1^T used as an outgroup. CD-HIT with a 0.4 protein sequence identity threshold was used for the determination. To further confirm the taxonomic distances, the OrthoANIu algorithm (Yoon et al., 2017b) and GGDC 2.1 (Meier-Kolthoff et al., 2013) were used to calculate the ANI and dDDH values of strains XCT-34^T and XCT-53 with other species.

The predicted protein sequences from the genomes of strains XCT-34^T, XCT-53, and their closest taxonomic relatives were submitted to BlastKOALA (http://www.kegg.jp/blastkoala/) for functional annotation based on KEGG orthology (Kanehisa et al., 2016) using the software's default parameters. The gene annotation results were presented in the form of numbers, with the numbers indicating the count of genes successfully annotated to that specific function. Putative secondary metabolites biosynthetic gene clusters (BGCs) were detected using antiSMASH (version 7.0.0) with default parameters (Blin et al., 2023), and the pathogenic characteristics were generated from the Pathogen-Host Interactions Database (PHI, version 5.0) (Urban et al., 2022).

Phenotypic, Physiological, and Biochemical Analyses

Considering their closeness to the two isolates in 16S rRNA similarity and phylogenomic analyses, *P. carbonis* Q4.6^T (KCTC 52466), *P. indicus* HT23^T (JCM 16851) and *P. phragmitetus* C6/19^T (DSM 14782) were purchased for parallel study respectively from the Korean Collection for Type Cultures (KCTC), Japan Collection of Microorganisms (JCM), and Deutsche Sammlung von Mikroorganismen und Zellkulturen GmbH (DSMZ).

Seven media [Reasoner's 2 agar (R2A), Brain–heart infusion (BHI) agar, Nutrient agar, tryptone soya agar (TSA), LB, Mac and Mueller–Hinton broth medium] were screened for optimal growth of the two strains, with R2A yielding the fastest growth. Then the effects of other conditions (with or without oxygen) on growth were evaluated by incubating on R2A for 2–4 days. Optimal growth conditions were determined using R2A at several temperatures (4, 10, 16, 28, 30, 35, 37, 42, 45, or 50 °C), eleven pH conditions (pH 3.0–13.0, at interval of 1.0 pH unit), and NaCl concentrations (0.5, 1.0, 2.0, 3.0, 4.0, 5.0, 6.0, 7.0, 8.0, 9.0, or 10.0% [*w/v*]). The following phenotypic experiments were performed using cells cultured under optimal growth conditions. Gram-staining was performed using the Color Gram 2 kit following the manufacturer's guidelines. Morphological features were observed under a transmission electron microscope and a light microscope using bacterial cells in the early log and stationary phase. Catalase reaction was determined using the ID Color Catalase kit, while oxidase and urease activities were tested using API reagents. Motility was tested by observing the spreading growth of bacterial cells after inoculation by piercing into semisolid (0.4%, [*w/v*] agar) R2A medium in test tubes.

To test carbon source utilization, acid production, enzyme activity from specific substrates, and additional physiological characteristics, the two newly isolated strains and their three closely related species were analyzed in parallel with API 50CH strips (suspended with API 50 CHB/E medium, for carbohydrate fermentation tests) and API ZYM tests (bioMérieux) following the manufacturer's instructions.

Cellular fatty acids were extracted from saponified and methylated material of each strain with the Sherlock automatic bacterial identification system and analyzed using gas chromatography. Respiratory quinones in XCT-34^T were analyzed by reverse phase high-performance liquid chromatography (HPLC), and polar lipids were analyzed by two-dimensional thin-layer chromatography (TLC).

GenBank Accession Numbers

The GenBank accession numbers for the nearly full-length 16S rRNA genes and genome sequences of strains XCT-34^T and XCT-53 are MN904904, MN905516, JAABLP000000000 and JAABLQ000000000, respectively. One Supplementary Table and six Supplementary Figures are available with the online Supplementary Materials.

Results and Discussion

16S rRNA Phylogeny

Analysis of 16S rRNA gene sequence-based identity revealed that strains XCT-34^T and XCT-53 were identical to each other, sharing high similarity with *P. carbonis* Q4.6^T (98.57%), *P. phragmitetus* C6/19^T (97.51%) and *P. indicus* HT23^T (97.29%). As shown in the three phylogenetic trees (Fig. 1; Figs. S1 and S2) constructed using 16S rRNA gene sequences from 34 closest related strains in EzTaxon database, strains XCT-34^T and XCT-53 were clustered together, forming an independent branch with members of the genus *Pannonibacter*, closest to *P. carbonis* Q4.6^T, *P. indicus* HT23^T and *P. phragmitetus* C6/19^T.

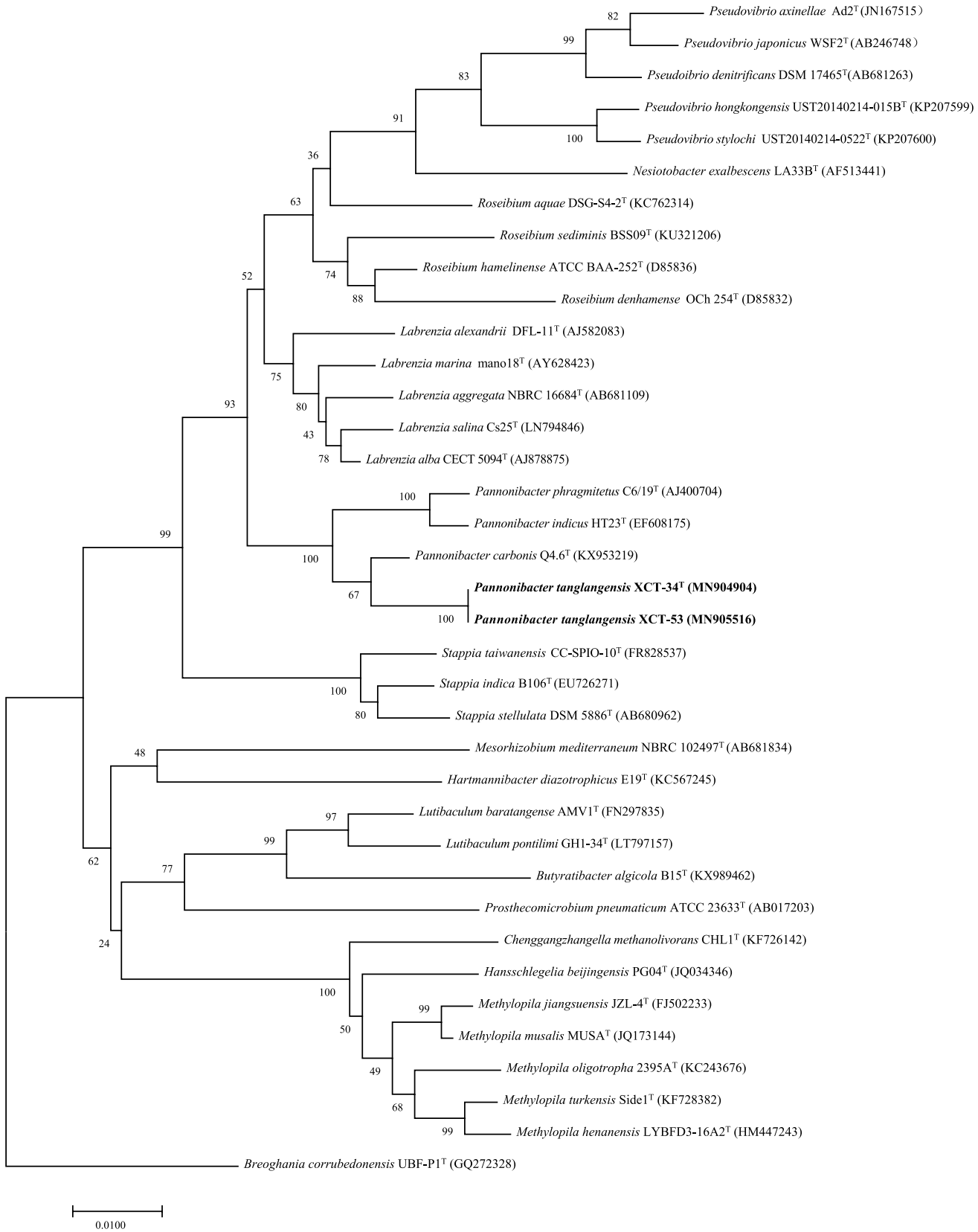

Fig. 1 Neighbour-joining tree based on the 16S rRNA gene. The tree shows the taxonomic position of strains XCT-34^T, XCT-53 and other closely related species. The numerals (values > 50% are noted) indicate percentage of bootstrap samplings as derived from 1000 replications. The sequence of *Breoghania corrubedonensis* UBF-P1^T serves as an outgroup. Bar, 0.01 substitutions per nucleotide position

Genome Characteristics

Devoid of plasmid, the whole genome of strain XCT-34^T (detailed in Table S1) consisted of a circular chromosome (4,588,697 bp long; 4263 genes; 4042 CDSs; 53 tRNA; 9 rRNA). Significantly, the DNA G + C contents of the two strains (67.2–67.3%) were higher than those of the other species (63.1–63.6%) in the genus *Pannonibacter*. The ANI and dDDH values between strains XCT-34^T and XCT-53 were 98.7% (higher than the 95–96% species threshold) and 95.3% (higher than the 70% species threshold), respectively, supporting that they were of the same species. By contrast, the ANI and dDDH values of the two strains against other strains in the genus *Pannonibacter* ranged from 85.7 to 86.4% and 22.3 to 30.5% (Table 1), both lower than the threshold for delineating species (Chun et al., 2018; Meier-Kolthoff et al., 2014; Richter & Rossello-Mora, 2009). The phylogenomic tree based on 945 core genes showed that strains XCT-34^T and XCT-53 formed a singular cluster within the genus *Pannonibacter* branch (Fig. 2), close to *P. carbonis* Q4.6^T, *P. indicus* HT23^T, and *P. phragmitetus* C6/19^T.

Table 1 Values of ANI and dDDH between strains XCT-34^T and XCT-53, and their closely related species

dDDH	ANI				
	1	2	3	4	5
XCT-34^T	–	98.7	86.4	81.1	81.2
XCT-53	95.3	–	85.7	81.2	81.3
1	22.3	30.5	–	80.9	80.9
2	22.1	22.1	21.7	–	93.6
3	22.0	22.0	21.7	50.0	–

Strains: 1, XCT-34^T; 2, XCT-53; 3, *P. carbonis* Q4.6^T; 4, *P. indicus* HT23^T; 5, *P. phragmitetus* C6/19^T

Genome Analyses

The distribution of genes in the KEGG functional categories indicated that the two new isolates and the other three *Pannonibacter* species had similar pathways in the global/overview maps and the energy metabolism, with similar numbers (32–35) of genes for flagellum synthesis (Pathway and module 02040 in Table 2 under 'Xenobiotics biodegradation and metabolism'). However, strains XCT-34^T and XCT-53 had more genes for bisphenol degradation, and nitrogen metabolism, whereas this transcriptional level was predicted to be less prevalent in their neighboring species. KEGG gene function analysis revealed that the two new isolates contained two putative pathways for biosynthesis of C5 and C10–C20 isoprenoids, which were absent in their neighboring species. By contrast, they lacked the putative pathways for biosynthesis of deoxyribonucleotide and pyrimidine deoxyribonucleotide, while their neighboring species had them. Taken together, the above genetic infrastructural differences between the two new isolates and their closely related species suggested their phenotypic stratification potentials.

Additional insights into the genome relatedness of ecological functions were investigated using the section of

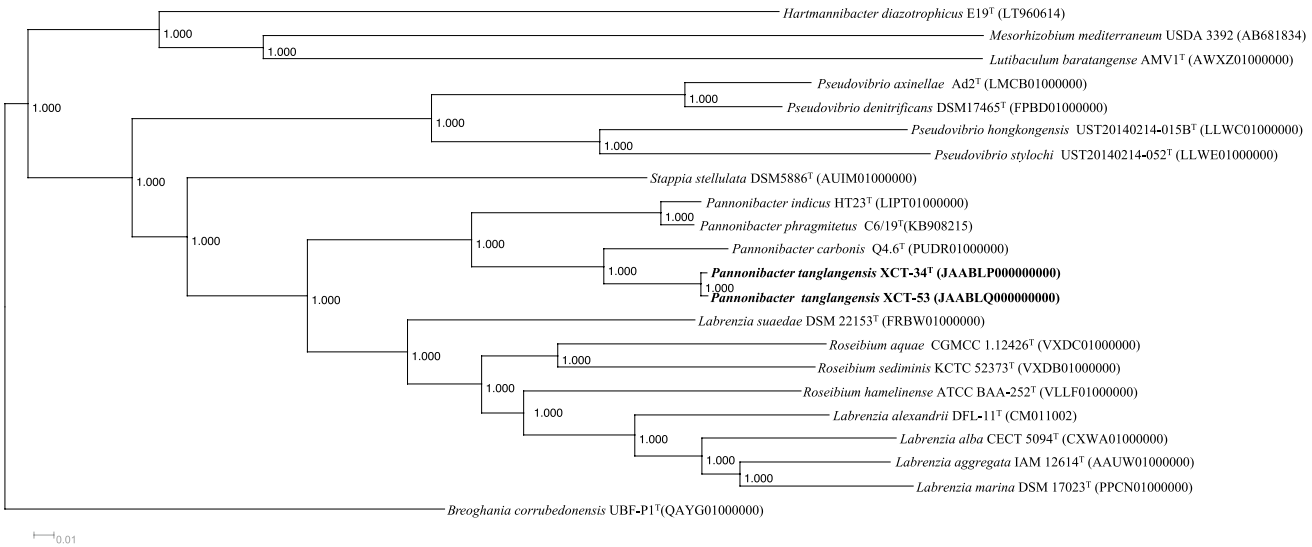

Fig. 2 Phylogenomic tree of *Pannonibacter* strains XCT-34^T, XCT-53, and closely related species. This tree is constructed based on 945 core genes from 20 genome sequences available on the GenBank database. The numbers in the tree indicate the reliability of each split with the Shimodaira-Hasegawa test calculated from 1000 resamples. The sequence of *Breoghania corrubedonensis* DSM 23382^T serves as an outgroup. Bar, 0.01 substitutions per nucleotide position

Table 2 Predicted differences of gene expression across six main categories in the KEGG database between the two novel strains and their neighboring strains

Pathway and Module	1	2	3	4	5
Pathway					
Global and overview maps					
01100 Metabolic pathways	688	680	686	687	710
01110 Biosynthesis of secondary metabolites	266	264	243	250	260
01120 Microbial metabolism in diverse environments	211	204	226	211	229
01200 Carbon metabolism	94	93	95	95	96
01210 2-Oxocarboxylic acid metabolism	21	21	21	21	21
01212 Fatty acid metabolism	18	19	20	20	20
01230 Biosynthesis of amino acids	95	93	93	96	96
01232 Nucleotide metabolism	38	39	39	39	39
01250 Biosynthesis of nucleotide sugars	28	27	28	29	33
01240 Biosynthesis of cofactors	126	122	125	124	129
01220 Degradation of aromatic compounds	14	14	16	13	25
Energy metabolism					
00190 Oxidative phosphorylation	47	47	46	51	51
00195 Photosynthesis	8	8	8	8	8
00710 Carbon fixation in photosynthetic organisms	13	12	12	12	12
00720 Carbon fixation pathways in prokaryotes	28	28	28	29	29
00680 Methane metabolism	24	22	22	21	22
00910 Nitrogen metabolism	12	7	20	16	21
00920 Sulfur metabolism	22	16	31	20	24
Glycan biosynthesis and metabolism					
00531 Glycosaminoglycan degradation	3	3	3	1	1
00604 Glycosphingolipid biosynthesis - ganglio series	1	1	1	0	0
00511 Other glycan degradation	3	2	2	1	1
00543 Exopolysaccharide biosynthesis	3	6	4	2	3
Biosynthesis of other secondary metabolites					
00960 Tropane, piperidine and pyridine alkaloid biosynthesis	4	4	2	2	3
00521 Streptomycin biosynthesis	7	4	4	4	8
00525 Acarbose and validamycin biosynthesis	2	0	0	0	2

environmental information processing in the KEGG database. Briefly, all strains exhibited a similar ecological functional pattern, with ATP-binding cassette (ABC) transporters and two-component signal transduction systems dominating (Fig. S3). AMP-activated protein kinase (AMPK), a serine threonine kinase highly conserved through evolution, acts as a sensor of cellular energy status and governs cell-autonomous adaptations during metabolic stress (Mahmoud et al., 2016). It is noteworthy that strains XCT-34^T and XCT-53 had no genes for AMPK signaling pathway, which were present in *P. indicus* HT23^T and *P. phragmitetus* C6/19^T. Considering that strains XCT-34^T and XCT-53 were motile (see below) with dominating presence of ABC transporters and two-component signal transduction systems in their environmental information processing, these properties definitely will give them the corresponding advantages when competing with other bacteria but their impact on sediment ecology remains to be seen.

All strains in Fig. 3 carried genes for synthesis of betalactones, proteusin and terpenes; when compared to the existing species, the synthetic gene numbers in strains XCT-34^T and XCT-53 were similar for betalactone, but far more for terpene and much less for proteusin (similar to *P. carbonis* Q4.6^T though). Regarding other biosynthetic gene clusters (BGCs), only *P. carbonis* Q4.6^T had BGCs for homoserine lactone. BGCs encoding for non-ribosomal peptide

Table 2 (continued)

Xenobiotics biodegradation and metabolism					
00627 Aminobenzoate degradation	6	6	7	5	10
00791 Atrazine degradation	3	3	3	5	4
00363 Bisphenol degradation	1	1	0	0	0
00983 Drug metabolism - other enzymes	13	13	13	12	12
02040 Flagellum synthesis	35	32	32	33	32
Completed module					
M00096 C5 isoprenoid biosynthesis	yes	yes	no	no	no
M00364 C10-C20 isoprenoid biosynthesis	yes	yes	no	no	no
M00053 Deoxyribonucleotide biosynthesis	no	no	yes	yes	yes
M00938 Pyrimidine deoxyribonucleotide biosynthesis	no	no	yes	yes	yes
M00017 Methionine biosynthesis	no	no	no	yes	yes
M00579 Phosphate acetyltransferase-acetate kinase pathway	no	no	no	yes	yes
M00616 Sulfate-sulfur assimilation	no	no	yes	no	no
M00126 Tetrahydrofolate biosynthesis	yes	yes	no	no	yes
M00531 Assimilatory nitrate reduction	yes	no	yes	yes	yes
M00615 Nitrate assimilation	yes	no	yes	yes	yes
M00552 D-galactonate degradation	yes	no	no	yes	yes

Strains: 1, XCT-34^T; 2, XCT-53; 3, *P. carbonis* Q4.6^T; 4, *P. indicus* HT23^T; 5, *P. phragmitetus* C6/19^T. The numbers below each strain are the count of genes successfully annotated to that specific function

synthetase-independent, IucA/IucC-like siderophores, and N-acetylglutaminylglutamine amide (NAGGN) existed in *P. indicus* HT23^T and *P. phragmitetus* C6/19^T but absent in others. BGCs for synthesis of acyl-amino-acids, RiPP and type I polyketide synthase (T1PKS) were strikingly similar between the two novel isolates and *P. carbonis* Q4.6^T, in contrast to *P. indicus* HT23^T and *P. phragmitetus* C6/19^T, which was consistent with the strain closeness result returned by the program (top, Fig. 3). Summary of the PHI phenotypes indicated that they shared similar characteristics within pathogen groups, and the gene group associated with reduced virulence was abundant in all strains (Fig. S4).

Phenotypic, Physiological, and Chemotaxonomic Characteristics

Growth of strains XCT-34^T and XCT-53 was observed in R2A medium (optimum), 10–40 °C (optimum, 35–37 °C), pH 4.0–10.0 (optimum, pH 8.0), and with up to 4% NaCl (*w/v*; optimum, 0.5%). Under optimal growth conditions, both strains were aerobic (neither grew under anaerobic condition), Gram-stain-negative, motile with polar flagella, oxidase-negative, catalase-positive, and rod-shaped with an approximately size of 1.4–3.4 × 0.4–0.9 μm (Fig. S5). The colonies were ivory, circular, smooth with an entire margin.

Some of the key physiological and biochemical differences of our isolates with the type strains of the three existing species were summarized in Table 3 and highlighted below. The two new isolates were strictly aerobic, similar to *P. indicus* HT23^T, in sharp contrast to the facultatively anaerobic feature presented by the other two species (Table 3). They produced acid from D-mannose (weakly from potassium 5-keto-gluconate) but not from salicin, in sharp contrast to *P. carbonis* Q4.6^T, *P. indicus* HT23^T, and *P. phragmitetus* C6/19^T. $C_{18:}\omega 7c$ (72.6%) was the primary fatty acid in strains XCT-34^T and XCT-53 (Table 4), similar to their relatives in the genus but higher than *P. carbonis* Q4.6^T and *P. indicus* HT23^T (average, 65.7%) (Bandyopadhyay et al., 2013) and lower than *P. phragmitetus* C6/19^T (75.8%) (Borsodi et al., 2003). The sole respiratory quinone in XCT-34^T was Q-10, same as other species in the genus *Pannonibacter*. The polar lipids comprised diphosphatidylglycerol, phosphatidylcholine, phosphatidylethanolamine, phosphatidylglycerol, one or two unidentified aminolipid(s) and aminophospholipid(s), one unidentified lipid, and four or six unidentified phospholipids (Fig. S6). The polar lipid profiles of the novel strains differed from their close relatives by having more phospholipids and the presence of aminophospholipid(s) but lacking phosphatidyl serine in *P. phragmitetus* C6/19^T (Borsodi et al., 2003) and phosphatidyl monomethyl ethanolamine in *P. indicus* HT23^T (Bandyopadhyay et al., 2013).

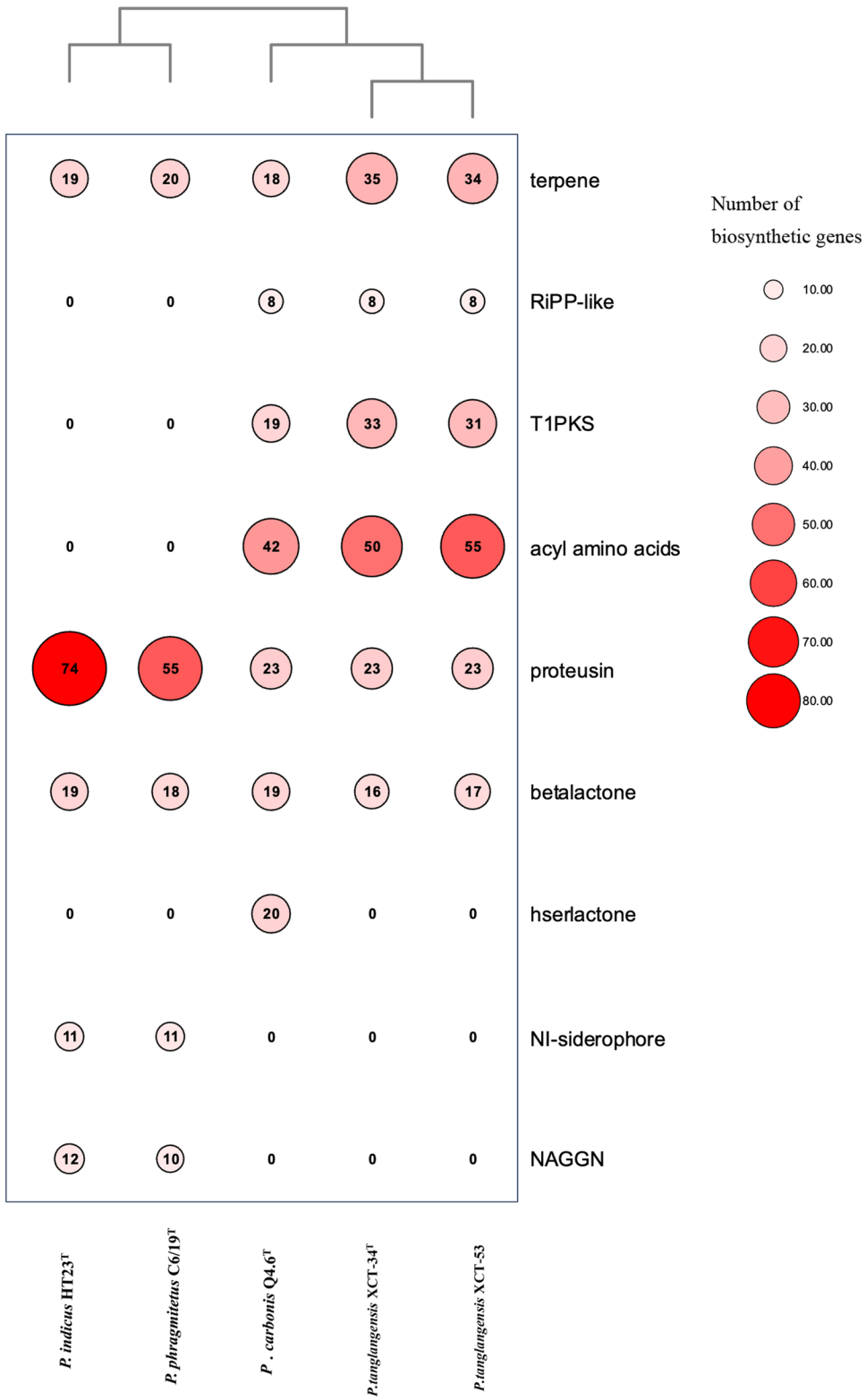

Fig. 3 Secondary metabolite biosynthetic genes identified in *Pannonibacter* strains using antiSMASH version 7.0.0

Taxonomic Conclusion

In conclusion, the phenotypic, phylogenetic, biochemical, chemotaxonomic, and genomic findings provided sufficient evidence to distinguish our two isolates from their closely related type strains of the other species of the genus. These results reveal that the two isolates (XCT-34^T and XCT-53) represent one novel species of the genus *Pannonibacter*,

Table 3 Phenotypic characteristics that differentiate strains XCT-34^T and XCT-53 from their closely related species

Characteristics	1	2	3	4	5
Temperature range (°C, optimum)	10–40 (35–37)	10–40 (35–37)	4–55 (30–35)	15–45 (30–37)	15–45 (30–37)
NaCl (%, *w/v*) tolerance	4	4	5.5	5	5
pH range for growth	4–10	4–10	3.5–10	3–9	3–9
Oxygen for growth	Strictly aerobic	Strictly aerobic	Facultatively anaerobic	Strictly aerobic	Facultatively anaerobic
Production of					
α-Chymotrypsin	w	−	−	−	−
Cystine arylamidase	w	−	−	−	−
Valine arylamidase	+	w	w	w	w
Acid production from					
Potassium 5-keto-gluconate	w	w	−	−	−
D-Mannose	+	+	w	w	w
Salicin	−	−	w	w	+
D-Arabinose	w	w	+	+	+
D-Xylose	+	+	w	−	−

Strains: 1, XCT-34^T; 2, XCT-53; 3, *P. carbonis* Q4.6^T; 4, *P. indicus* HT23^T; 5, *P. phragmitetus* C6/19^T. +, positive. w, weakly positive. −, negative. All data were from this study

Table 4 Fatty acid contents (%) of strains XCT-34^T and XCT-53, and their closely related species

Fatty acid	1	2	3	4[a]	5[b]
$C_{14:0}$ 3OH/iso-$C_{16:1}$	8.5	6.9	3.7	3.4	1.3
$C_{16:0}$	3.7	4.5	7.3	7.2	6.5
$C_{18:0}$	2.9	2.2	7.5	8.7	1.6
$C_{18:0}$ 3OH	2.4	3.1	3.2	2.2	2.2
$C_{18:1}\omega7c$	72.4	72.8	68.4	62.9	75.8
11-methyl $C_{18:1}\omega7c$	0.9	1.1	2.0	7.4	9.9
Cyclo-$C_{19:0}\omega10c$/19$\omega6$	5.3	6.5	2.0	0.7	0.6
Summed Feature 2	9.4	8.2	4.2	NA	NA

Strains: 1, XCT-34^T; 2, XCT-53; 3, *P. carbonis* Q4.6^T; 4, *P. indicus* HT23^T; 5, *P. phragmitetus* C6/19^T

NA data not available

[a]Data from Bandyopadhyay et al. (2013)

[b]Data from Borsodi et al. (2003)

for which the name *Pannonibacter tanglangensis* sp. nov. is proposed.

Description of *Pannonibacter tanglangensis* sp. nov.

Pannonibacter tanglangensis (tang.lang.en´sis. N.L. masc. adj. *tanglangensis* referring to the Tanglang mountain in Shenzhen of China where this species was isolated from).

Cells are aerobic, Gram-stain-negative, oxidase-negative, catalase-positive, motile with polar flagella, rod-shaped, approximately 1.4–3.4 × 0.4–0.9 μm in size. After growth on R2A agar for 2 days at 35 °C, colonies are ivory, circular, smooth with an entire margin. Growth occurs on R2A at 10–40 °C (optimum, 35–37 °C), at pH 4.0–10.0 (optimum, pH 8.0), and with up to 4% NaCl (*w/v*; optimum, 0.5%). In the API 50CH strip, acid is produced from D-fructose, D-fucose, D-glucose, D-mannose, D-xylose, L-fucose, maltose, polychrome esculine citrate, sucrose, and trehalose, and weakly produced from D-arabinose, D-galactose, D-ribose, D-turanose, cellobiose, glycerol, inositol, L-arabinose, melibiose, *N*-acetyl-glucosamine, and potassium 5-keto-gluconate, but not produced from amygdaline, arbutin, D-adonitol, D-arabitol, D-mannitol, D-sorbitol, D-tagatose, dulcitol, erythritol, gentiobiose, glycogen, inulin, lactose, L-arabitol, L-rhamnose, L-sorbose, L-xylose, melezitose, methyl *α*-D-glucopyranoside, methyl α-D-mannopyranoside, methyl *β*-D-xylopyranoside, potassium gluconate, potassium 2-keto-gluconate, raffinose, salicin, starch, and xylitol. In the API ZYM strip, positive for acid phosphatase, alkaline phosphatase, esterase (C4), esterase lipase (C8), leucine arylamidase, naphthol-AS-BI-phosphohydrolase, phosphohydrolase, trypsin, valine arylamidase, *α*-galactosidase, *β*-galactosidase, *β*-glucosidase, and *β*-glucuronidase; weakly positive for *α*-glucosidase; variable for cystine arylamidase, and *α*-chymotrypsin, but negative for lipase (C14), *N*-acetyl-*β*-glucosaminidase, and *α*-mannosidase. The major fatty acid is $C_{18:}\omega7c$, and the principal respiratory quinone is Q-10. Polar lipids include diphosphatidylglycerol, phosphatidylcholine, phosphatidylethanolamine, phosphatidylglycerol, 1–2 unidentified aminolipid(s), 1–2 unidentified aminophospholipid(s), one unidentified lipid, and 4–6 unidentified phospholipids.

The type strain, XCT-34^T (= KCTC 82332^T = GDMCC 1.1947^T), with a genomic DNA G + C content of 67.2%, was isolated from an artificial freshwater reservoir near the

Tanglang mountain in Shenzhen of China. The GenBank accession numbers for the 16S rRNA gene and genome sequences of strains XCT-34^T/XCT-53 are MN904904/MN905516 and JAABLP000000000/JAABLQ000000000, respectively.

Supplementary Information The online version contains supplementary material available at https://doi.org/10.1007/s12275-024-00151-y.

Acknowledgements This work was supported by the Sanming Project of Medicine in Shenzhen (SZSM202311015), Shenzhen Science and Technology Innovation Committee (JCYJ20230807151802005), and the Shenzhen Key Medical Discipline Construction Fund (SZXK064).

Data availability The data that support the findings of this study are openly available in GeneBank at https://www.ncbi.nlm.nih.gov/.

Declarations

Conflict of interest The authors declare no conflict of interest.

References

Bandyopadhyay, S., & Das, S. K. (2016). Functional analysis of ars gene cluster of *Pannonibacter indicus* strain HT23^T (DSM 23407^T) and identification of a proline residue essential for arsenate reductase activity. *Applied Microbiology and Biotechnology, 100*, 3235–3244.

Bandyopadhyay, S., Schumann, P., & Das, S. K. (2013). *Pannonibacter indica* sp. nov., a highly arsenate-tolerant bacterium isolated from a hot spring in India. *Archives of Microbiology, 195*, 1–8.

Blin, K., Shaw, S., Augustijn, H. E., Reitz, Z. L., Biermann, F., Alanjary, M., Fetter, A., Terlouw, B. R., Metcalf, W. W., Helfrich, E. J. N., et al. (2023). antiSMASH 7.0: New and improved predictions for detection, regulation, chemical structures and visualisation. *Nucleic Acids Research, 51*, W46–W50.

Borsodi, A. K., Micsinai, A., Kovács, G., Tóth, E., Schumann, P., Kovács, A. L., Böddi, B., & Márialigeti, K. (2003). *Pannonibacter phragmitetus* gen. nov., sp. nov., a novel alkalitolerant bacterium isolated from decomposing reed rhizomes in a Hungarian soda lake. *International Journal of Systematic and Evolutionary Microbiology, 53*, 555–561.

Chun, J., Oren, A., Ventosa, A., Christensen, H., Arahal, D. R., da Costa, M. S., Rooney, A. P., Yi, H., Xu, X. W., De Meyer, S., et al. (2018). Proposed minimal standards for the use of genome data for the taxonomy of prokaryotes. *International Journal of Systematic and Evolutionary Microbiology, 68*, 461–466.

Delgado, S., Suárez, A., & Mayo, B. (2006). Identification of dominant bacteria in feces and colonic mucosa from healthy Spanish adults by culturing and by 16S rDNA sequence analysis. *Digestive Diseases and Sciences, 51*, 744–751.

Gallardo, A., Merino Bueno, M. D. C., Sango Merino, C., Suárez Laurés, A. M., de la Torre-Fernández, M., & Sánchez Álvarez, E. (2020). First case of bacteriemia caused by *Pannonibacter phragmitetus* in a haemodialysis patient. *Nefrología, 42*, 209–210.

Holmes, B., Segers, P., Coenye, T., Vancanneyt, M., & Vandamme, P. (2006). *Pannonibacter phragmitetus*, described from a Hungarian soda lake in 2003, had been recognized several decades earlier from human blood cultures as *Achromobacter* groups B and E. *International Journal of Systematic and Evolutionary Microbiology, 56*, 2945–2948.

Huson, D. H., & Scornavacca, C. (2012). Dendroscope 3: An interactive tool for rooted phylogenetic trees and networks. *Systematic Biology, 61*, 1061–1067.

Jin, D., Chen, C., Li, L., Lu, S., Li, Z., Zhou, Z., Jing, H., Xu, Y., Du, P., Wang, H., et al. (2013). Dynamics of fecal microbial communities in children with diarrhea of unknown etiology and genomic analysis of associated *Streptococcus lutetiensis*. *BMC Microbiology, 13*, 141.

Kanehisa, M., Sato, Y., Kawashima, M., Furumichi, M., & Tanabe, M. (2016). KEGG as a reference resource for gene and protein annotation. *Nucleic Acids Research, 44*, D457–D462.

Kimura, M. (1980). A simple method for estimating evolutionary rates of base substitutions through comparative studies of nucleotide sequences. *Journal of Molecular Evolution, 16*, 111–120.

Kumar, S., Stecher, G., & Tamura, K. (2016). MEGA7: Molecular evolutionary genetics analysis version 7.0 for bigger datasets. *Molecular Biology and Evolution, 33*, 1870–1874.

Lagesen, K., Hallin, P., Rødland, E. A., Staerfeldt, H. H., Rognes, T., & Ussery, D. W. (2007). RNAmmer: Consistent and rapid annotation of ribosomal RNA genes. *Nucleic Acids Research, 35*, 3100–3108.

Liao, Q., Tang, J., Wang, H., Yang, W., He, L., Wang, Y., & Yang, Z. (2020). Dynamic proteome responses to sequential reduction of Cr(VI) and adsorption of Pb(II) by *Pannonibacter phragmitetus* BB. *Journal of Hazardous Materials, 386*, 121988.

Mahmoud, A. D., Lewis, S., Juričić, L., Udoh, U. A., Hartmann, S., Jansen, M. A., Ogunbayo, O. A., Puggioni, P., Holmes, A. P., Kumar, P., et al. (2016). AMP-activated protein kinase deficiency blocks the hypoxic ventilatory response and thus precipitates hypoventilation and apnea. *American Journal of Respiratory and Critical Care Medicine, 193*, 1032–1043.

Meier-Kolthoff, J. P., Auch, A. F., Klenk, H. P., & Goker, M. (2013). Genome sequence-based species delimitation with confidence intervals and improved distance functions. *BMC Bioinformatics, 14*, 60.

Meier-Kolthoff, J. P., Hahnke, R. L., Petersen, J., Scheuner, C., Michael, V., Fiebig, A., Rohde, C., Rohde, M., Fartmann, B., Goodwin, L. A., et al. (2014). Complete genome sequence of DSM 30083^T, the type strain (U5/41^T) of *Escherichia coli*, and a proposal for delineating subspecies in microbial taxonomy. *Standards in Genomic Sciences, 9*, 2.

Price, M. N., Dehal, P. S., & Arkin, A. P. (2009). FastTree: Computing large minimum evolution trees with profiles instead of a distance matrix. *Molecular Biology and Evolution, 26*, 1641–1650.

Richter, M., & Rosselló-Móra, R. (2009). Shifting the genomic gold standard for the prokaryotic species definition. *Proceedings of the National Academy of Sciences, 106*, 19126–19131.

Saravanan, A., Kumar, P. S., Yaashikaa, P. R., Karishma, S., Jeevanantham, S., & Swetha, S. (2021). Mixed biosorbent of agro waste and bacterial biomass for the separation of Pb(II) ions from water system. *Chemosphere, 277*, 130236.

Shi, Y., Chai, L., Yang, Z., Jing, Q., Chen, R., & Chen, Y. (2012). Identification and hexavalent chromium reduction characteristics of *Pannonibacter phragmitetus*. *Bioprocess and Biosystems Engineering, 35*, 843–850.

Tamura, K., Stecher, G., & Kumar, S. (2021). MEGA11: Molecular evolutionary genetics analysis version 11. *Molecular Biology and Evolution, 38*, 3022–3027.

Urban, M., Cuzick, A., Seager, J., Wood, V., Rutherford, K., Venkatesh, S. Y., Sahu, J., Iyer, S. V., Khamari, L., De Silva, N., et al. (2022). PHI-base in 2022: A multi-species phenotype database for pathogen–host interactions. *Nucleic Acids Research, 50*, D837–D847.

Xi, L., Qiao, N., Liu, D., Li, J., Zhang, J., & Liu, J. (2018). *Pannonibacter carbonis* sp. nov., isolated from coal mine water. *International Journal of Systematic and Evolutionary Microbiology, 68*, 2042–2047.

Yoon, S. H., Ha, S. M., Kwon, S., Lim, J., Kim, Y., Seo, H., & Chun, J. (2017a). Introducing EzBioCloud: A taxonomically united database of 16S rRNA gene sequences and whole-genome assemblies. *International Journal of Systematic and Evolutionary Microbiology, 67*, 1613–1617.

Yoon, S. H., Ha, S. M., Lim, J., Kwon, S., & Chun, J. (2017b). A large-scale evaluation of algorithms to calculate average nucleotide identity. *Antonie Van Leeuwenhoek, 110*, 1281–1286.